Springer

Journal of Mechanical Science and Technology 23 (2009) 2376~2389

Journal of Mechanical Science and Technology

www.springerlink.com/content/1738-494x
DOI 10.1007/s12206-009-0628-5

Reverse flow in a square duct with an obstruction at the entry †

Chang-Hyun Sohn*, B. H. Lakshmana Gowda and Myong-Gun Ju

School of Mechanical Engineering Kyungpook National University Daegu, Korea 702-701

(Manuscript Received July 10, 2008; Revised October 30, 2008; Accepted May 19, 2009)

Abstract

In this paper, the reverse flow in a square duct with an obstruction at the front (which is a square plate), is investigated using particle image velocimetry (PIV). The gap g between the obstruction and the entry to the duct was systematically varied, and it was found that maximum reverse flow occurs around a g/w value of 0.75. The velocity vectors, vorticity plots, and other details described indicate that the flow field is different compared with the two-dimensional channel case.

Keywords: Reverse flow; Square duct; Obstruction; Shear layers; PIV

1. Introduction

Reverse flow (i.e., flow opposite to the direction of the free stream) inside a channel occurs when an obstruction is placed at certain positions near the entry of a channel, which is placed in another wider channel. The configuration for the realization of the reverse flow is shown in Fig. 1. When the gap between the obstruction and the channel entry is sufficiently large, forward flow results, but its magnitude even for large gap widths will be less than the free stream velocity U_∞.

Some applications in which reverse flow phenomena occurs or can be employed are control of flow, especially to obtain low velocities; heat transfer problems, where it may be required to have different types of flows locally; interaction of shear layers at different distances apart; and flow past obstruction/constriction in arterial flows under certain physiological situations [1]. It should be pointed out that the flow field will be more complex in arterial flows due to the elastic nature of the arteries.

Gowda and Tulapurkara [2] appear to have been the first researchers to observe the reverse flow phenomenon inside a channel. They studied the influence of gap (g), the length of the test channel (L), and the Reynolds number (Re) based on the channel width (w) and the free stream velocity U_∞. They observed that the maximum reverse flow occurs for a g/w = 1.5 and the stagnant flow condition happens for a g/w = 3.5.

As the Reynolds number increases, the reverse flow increases. Gowda and Tulapurkara also conducted both flow visualization and pressure measurements in a wind tunnel to examine whether the aforementioned features, which were observed at low Reynolds numbers, also occur at high Reynolds numbers. The experiments were carried out at Re = 26,000. The reverse flow velocity results obtained from these measurements show that the behavior of $-U_i/U_\infty$ exhibits trends similar to those at lower Reynolds numbers.

Gowda et al. [3] investigated the influence of the geometry of the obstruction using different shapes like squares, circles, triangles, and semicircles. A maximum reverse flow of $(U_i/U_\infty) = 0.28$ was obtained for the obstruction with a triangular shape. The effects of obstructions both at the entry and at the rear

† This paper was recommended for publication in revised form by Associate Editor Dongshin Shin

*Corresponding author. Tel.: +82 53 950 5570, Fax.: +82 53 950 6550
E-mail address: chsohn@knu.ac.kr

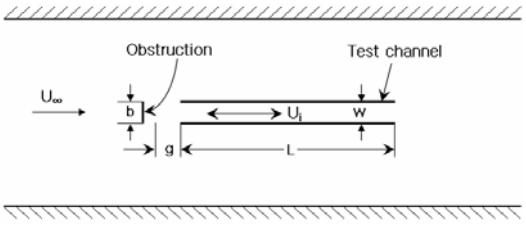

Fig. 1. Realization of reverse flow.

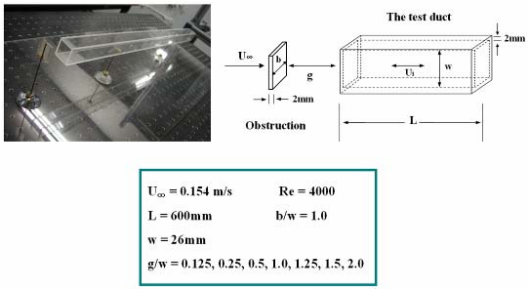

Fig. 2. Experimental arrangement.

end of the test channel were investigated by Tulapurkara et al. [4]. Studies were carried out by placing flat plates and semicircular scoops at the rear end (normal to the channel axis) in addition to the obstruction at the front end. Using semicircular scoops at the rear end and a flat plate at the front end, a maximum reverse flow of 83% of the free stream velocity was achieved. Gowda et al. [5] investigated the influence of splitter plates a) when placed at the front end and b) when placed at the rear end. For the latter, a maximum reverse flow of 37% of the free stream velocity was obtained. Gowda et al. [6] examined the mechanism behind the reverse flow phenomenon by conducting both flow visualization and pressure measurements. Flow visualization studies by Kabir et al. [7, 8] cover a range of Reynolds numbers up to 9,000. They confirmed the results found by Gowda and Tulapurkara [2] that the reverse flow is at its maximum value for the ratio of g/w = 1.5. Bhuiyan et al. [1] observed that the reverse flow also occurs in non-Newtonian fluid flows.

In the present study, the reverse flow phenomenon in a square duct is investigated. Unlike a two-dimensional plate (as in the case of a channel), the obstruction is a square plate. The flow features are different compared with the channel as the study deals with duct flow and a square plate as the obstruction. The flow at the rear end where the shear layers interact to generate the reverse flow are also different because the flow there is three-dimensional.

2. Experimental arrangement

All the experiments were carried out in the Flow Visualization Facility at the School of Mechanical Engineering, Kyungpook National University, Korea. Made out of acrylic sheets to ensure transparency, the flow visualization tank consists of a tank 2.5 m x 1.5 m with a depth of 0.3 m. It is filled with water to a depth of 200 mm. At one end of the tank two sets of aluminum discs (vanes) with suitable spacing in between them are located. The vanes, when rotated, act as paddles and create the flow in the test section. A variable speed D.C. motor with suitable gear arrangement is used to rotate the vanes, thus a wide range of flow speeds can be achieved in the test section. The flow is guided into the test section through suitably designed guide blocks. By varying the speed of rotation, the velocity in the test section can be varied up to 0.2 m/s without any wavy oscillations in the flow. Figure 2 shows the details of the square duct used for the reverse flow studies with the obstruction (a square plate; b/w = 1), as well as the various dimensions used in the test setup. The square duct and the square plate obstruction are fixed on a base plate. The base plate is inverted and then placed and supported on the guide blocks. This was done so that the struts supporting the duct and the obstruction do not interfere with the view, as the camera for the particle image velocimetry (PIV) studies and visualization are located below the tank (Figs. 3-4). The duct is located midway in the channel, below the water level, with its center line 100 mm from the water surface. The gap g between the entry to the duct and the obstruction is systematically varied to get g/w values of 0.125, 0.25, 0.5, 1.0, 1.25, 1.5, and 2.0.

A PIV system consisting of a 3 watt Ar-Ion Laser (Fig. 3) is used to measure velocities. The seeding was done using highly porous polymer particles sized 80-200 μm. A Readlake MotionPro X3 High-speed CCD camera (1280x1024 pixel) was used to record the flow details at 150 frames/sec (fps), and the particle images were processed using a proVISION package. Figure 4 shows the photograph of the test setup with the PIV system. As previously mentioned, the camera is located below the tank, normal to the laser sheet (Fig. 4).

The results presented are at a Reynolds number of 4000, referred to as the free stream velocity and the

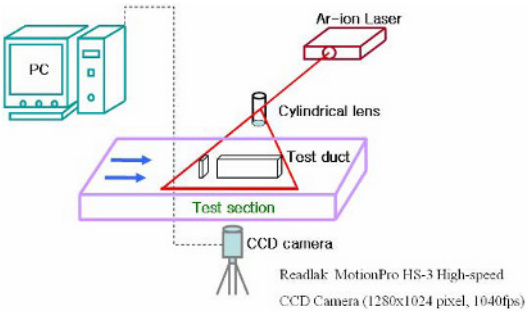

Fig. 3. PIV system.

(a) Ar-Ion Laser (3w)

(b) PIV experimental apparatus

Fig. 4. Photograph of the test setup.

width of the duct. The free stream velocity is uniform up to a distance of three times the width of the duct on either side of the duct center line, both in the horizontal and the vertical planes, with the variation being less than 2%. Results are obtained at another Reynolds number of 2,600 in order to compare reverse flow magnitudes. The measurements are also done at cross sections along various heights of the duct (Fig. 5). This was necessary as the experiment deals with a three-dimensional flow field.

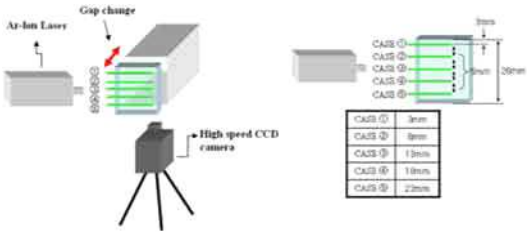

Fig. 5. Tests at cross sections at various heights.

3. Results

The velocity vectors and the vorticity contours along the channel for different g/w values are shown in Figs. 6(a) to f (results for g/w = 0.25 and 1.25 are not shown). In each figure, two parts representing the two portions of the duct (the front and the rear) are shown with a small gap at the center to accommodate the important features at the front and the rear ends. The gap is present to indicate that the flow pattern shown at the right half of the figure does not occur immediately downstream of the flow shown at the left half. In each figure, care has been taken to retain the essential features of the flow at both ends of the duct.

Reverse flow is clearly seen at g/w = 0.125 (Fig. 6(a)). The flow enters at the rear end and the vectors indicate that this flow impinges on the obstruction at the front end and exits through the gap between the duct entry and the obstruction. The vectors indicate the flow pattern and the recirculation regions at the rear and front ends. The vorticity plot (given below the vector plot) reveals the concentration of vorticity at the corresponding positions at the rear end and near the two sides of the duct at the front. Further, the vortical patterns are nearly symmetrical. At the rear end, there appears to be a stagnation point that is located nearly along the center line of the duct, with the flow almost symmetrical with respect to the two sides of the duct.

With increase in g/w (Figs. 6b-6c), the reverse flow intensifies and the flow pattern and the vorticity contours become similar to those in Fig. 6a. However, the stagnation point formed between the forward flow and the reverse flow at the exit, slightly away from

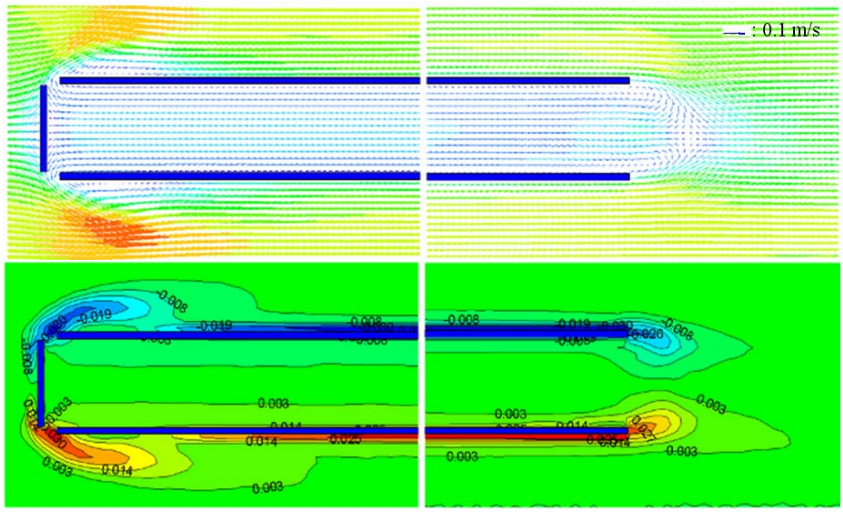

(a) g/w = 0.125

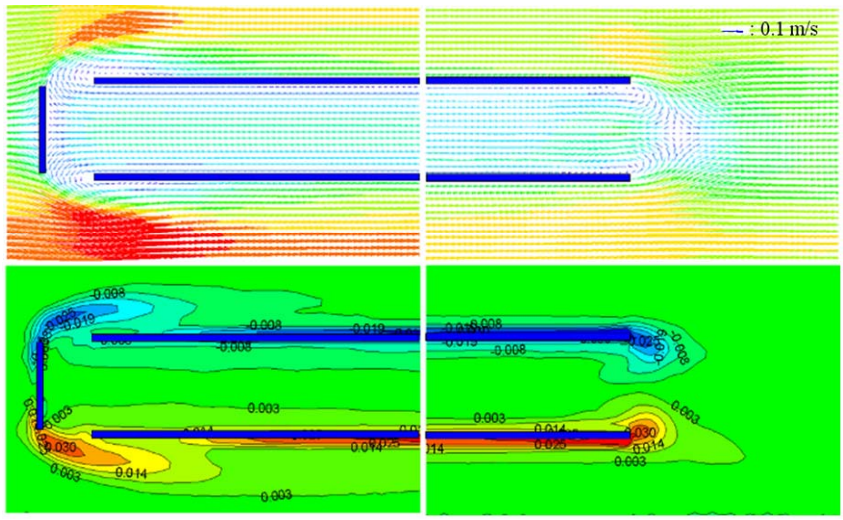

(b) g/w = 0.5

Fig. 6. Velocity vectors and vorticity contours for different g/w ratios (Re = 4,000).

the rear end, alters its position with g/w. (This aspect will be referred to later while discussing Fig. 13).

At g/w = 1.5 (Fig. 6(d)), the velocity vectors at the front end show that the gap between the obstruction and the duct entry is just sufficient enough to permit the rolling up of the separated shear layers originating from the edges of the obstruction, which is also reflected in the vorticity contours. Vortical regions are created at the front end, the positions of which can be expected to affect the reverse flow magnitude. This is what happens as indicated by the magnitude of the reverse flow velocity, shown in Fig. 7. At g/w = 1.75 (Fig. 6(e)), it was observed that the flow alternates between very weak reverse/forward flow, but overall the conditions could be described as stagnant. As shown by the vector plot and the vorticity contours, the vortical flow behind the obstruction for this value of g/w has an effect of "sealing" the entrance to the duct, thus giving rise to stagnant conditions. A further increase in the gap (g/w = 2; Fig. 6(f)) makes the gap between the obstruction and the entry to the duct large enough to permit the rolling up of the shear layers behind the square plate. There is sufficient space between the rolled-up shear layers and the duct

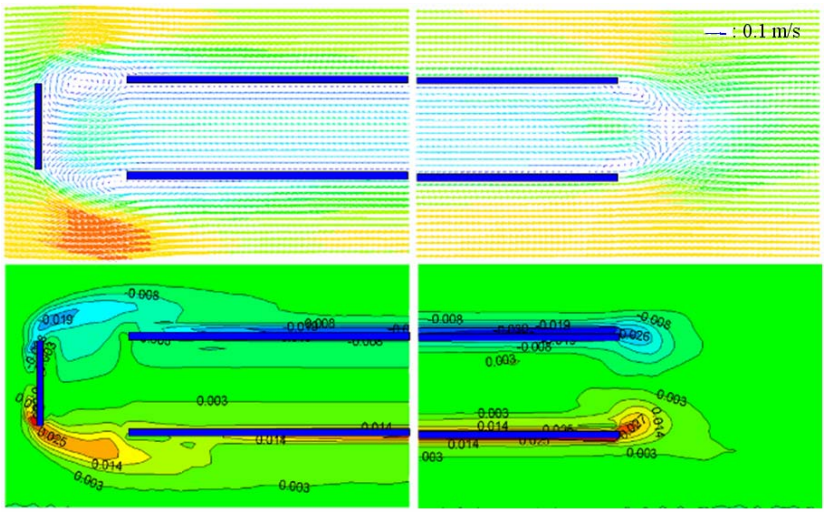

(c) g/w = 1.0

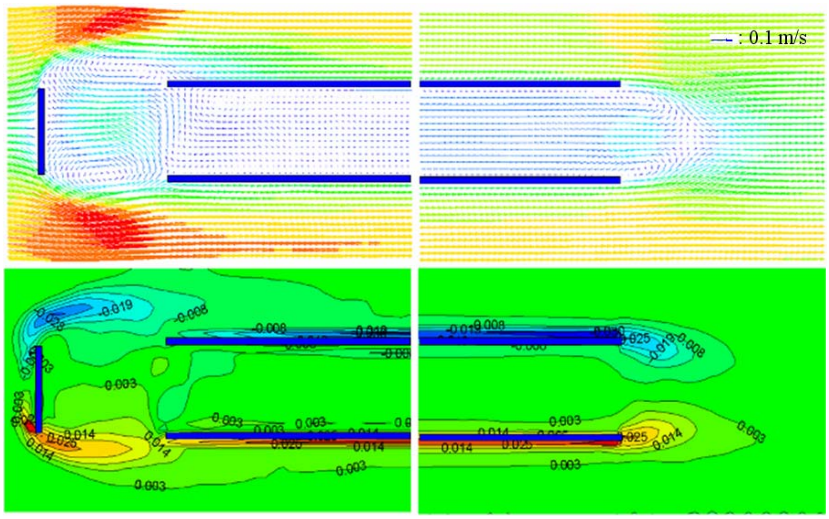

(d) g/w = 1.5

Fig. 6. Velocity vectors and vorticity contours for different g/w ratios (Re = 4,000; continued).

entry, which results in forward flow. In each of these cases (Figs. 6(d)-6(f)), the vorticity patterns on either side at the rear end are nearly symmetrical, as shown Figs. 6(a)-6(c). The significance of this symmetry is discussed in a later section.

The reverse flow magnitudes (measured at the central section) at various values of g/w are shown in Fig. 7. The magnitude of the velocity was expressed as a ratio of velocity, U_i, in the central part of the test channel to the free stream velocity, U_∞. In this figure, the results for a circular duct [9] and a channel [2] are shown for comparison. In the square duct, the variation is different from the two-dimensional channel case. The maximum reverse flow velocity occurs at a g/w of about 0.75 at a Reynolds number of 4,000, and its magnitude (U_i/U_∞ = -0.50) is nearly twice that for the two-dimensional case. In addition, the forward flow occurs at a much lower value of g/w (about 2) compared with that for the two-dimensional case (about 4) [6]. However, there are similarities between the present and the circular duct cases [9]. The possible reasons for these observed features are discussed in the next section.

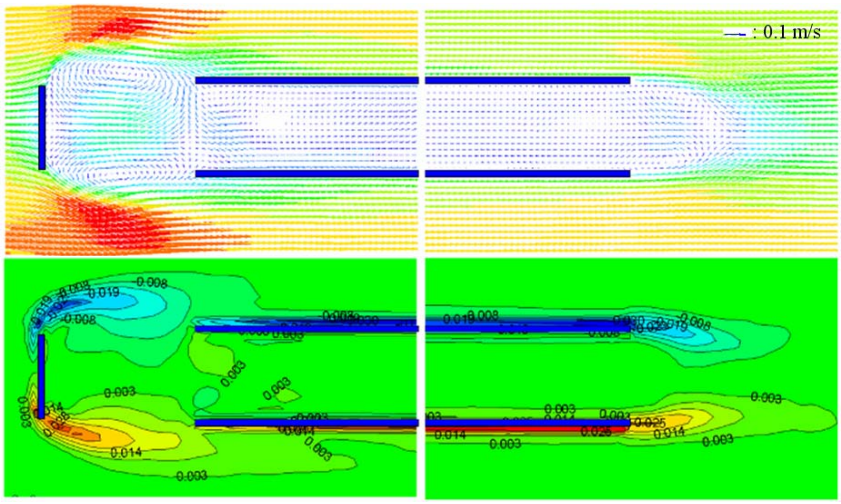

(e) g/w = 1.75

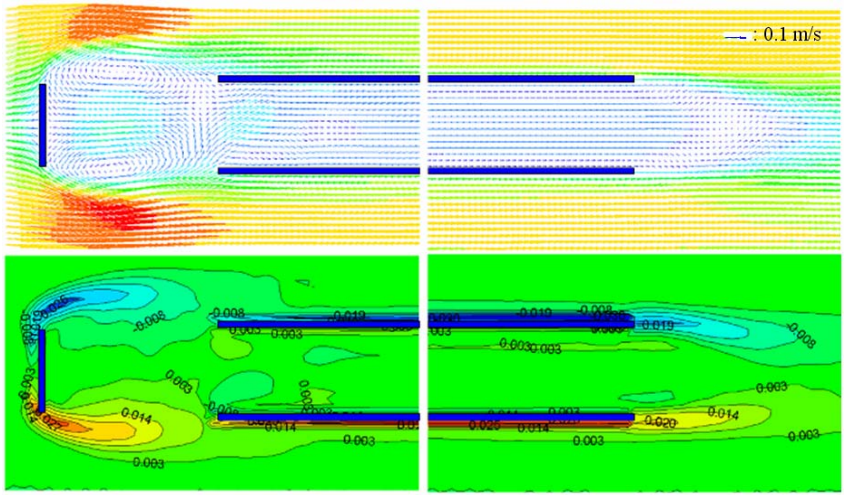

(f) g/w = 2.0

Fig. 6. Velocity vectors and vorticity contours for different g/w ratios (Re = 4,000; continued).

4. Discussion

Reverse flow in the case under study is expected to be triggered due to the low pressure behind the obstruction as in the channel case [2]. The primary reason for the differences observed between the two cases (i.e., the square duct and the channel) is the difference in geometry: the present case is three-dimensional and the channel case is two-dimensional. The effect is clearly seen when the flow at the rear end is considered (Fig. 6). The shear layer interaction seen in Fig. 6 is different from that for the channel [2]. The absence of vortical or recirculating separated regions within the duct near the rear and the front ends in Fig. 6 should be noted. There is very little periodicity at the two ends, particularly at the rear end, which is unlike the case of two-dimensional geometry [2]. In the latter case, there is vortex formation at the rear end and alternate pumping of the fluid into the channel. However, in the present case, no such alternating vortical activity is seen and the reverse flow is generated by the continuous rolling up of the shear layers into the channel. Moreover, the flow enters from all sides because the geometry is three-dimensional. This appears to be the reason for the increased reverse-flow magnitude in the present case,

U_i/U_∞ = -0.50 compared with -0.2 in the channel case.

To obtain a better physical picture of the flow patterns with time, and to check whether the flow is periodic or not, a series of photographs was taken at intervals of $1/8^{th}$ of a second over a period of several seconds. These should reveal whether periodicity exists. A typical set of photographs is presented in Figs. 8(a)-8(e). The figures show the streak lines that indicate the flow pattern at specific periods. To limit the number of photographs to be presented in a single figure, flow field is presented at intervals of $2/8^{th}$ of a second over a 1-second period. As shown in Figs. 8(a) to (e), there is hardly any periodicity in the flow at the rear end, which is very much contrary to the result in the channel case [2]. As mentioned previously, in the latter case, vortices are formed alternately at the rear end, which pump the fluid into the channel, thus generating the reverse flow. However, in the present case, there appears to be a continuous flow in the reverse direction into the duct from all sides. This is also the reason for the nearly symmetrical patterns of the vorticity distributions on either side of the mid-section seen in Figs. 6(a)-6(f), which was pointed out in the previous section.

When dealing with the flow in a square duct, the flow can be expected to vary across the height of the duct. Due to the finiteness of the square duct, three-dimensional effects can exist, which may influence the flow field at different heights from the center line of the duct. To investigate further, the flow patterns at cross sections other than at the center, at various heights h (Fig. 5) were carried out. These results are shown in Figs. 9(a)-9(d). The figures show that the flow field (velocity vectors and vorticity patterns) at various heights do not display any periodicity and that there is a continuous flow into the duct. It is surprising that there is very little variation across the height of the duct. It is probable that the duct corner effects are limited to a very small region. The flow at the rear end is akin to a "vortex ring"-like flow.

The other observed difference between the present case and the two-dimensional channel case in Fig. 7 is in the value of the g/w where the reverse flow ceases and forward flow results. This is mostly due to the geometry of the obstruction and the flow behind it. The recirculation region behind a square plate can be expected to be much shorter (due to the three-dimensional relief effect) than that for a two-dimensional plate. This is evident when the results in Fig. 6 are compared with the corresponding flow

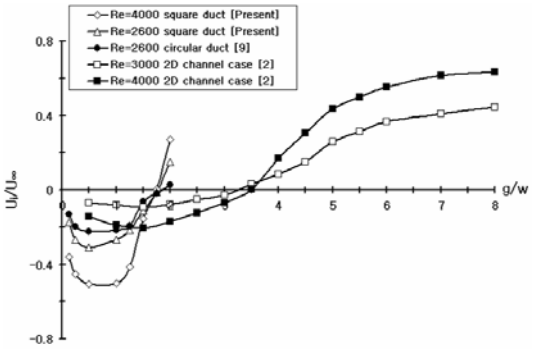

Fig. 7. Magnitude of reverse flow velocity at various gaps.

patterns for the channel case [2]. As shown in Figs. 6(a)-6(d), the reverse flow starts, intensifies, and persists as long as the shear layers separating from the edges of the obstruction at the front extend to the sides of the duct; this is indicated by both the vectors and the vorticity patterns. At g/w = 1.5, there is just enough space between the obstruction and the duct entry for the shear layers to roll up, which causes a reduction in the magnitude of the reverse flow. At a slightly higher value of g/w (1.75), the rolled-up shear layers almost block the entrance to the duct and a stagnant condition results. However, in the case of the two-dimensional channel, such situation occurs at a g/w of 3.5 [2]. Thus, in the case of the square plate obstruction, the shear layers behind can roll up and influence the flow in the gap between the plate and the entry to the duct at a comparatively lower value of g/w than for a two-dimensional flat plate obstruction in front of a channel. This roll-up would, in turn, act as a type of brake or resistance to the reverse flow and thus reduce its value, eventually giving rise to stagnant conditions. From the same line of argument, forward flow also starts earlier in the duct for the square geometry (at g/w =2) compared with the two-dimensional case (at g/w = 4 [2]), Fig. 7. At a much smaller gap compared with the channel case, there will be enough space between the recirculating eddy behind the square plate obstruction and the duct entrance for the forward flow to begin in the duct.

The aforementioned flow conditions at the front end as g/w is varied can be expected to have a corresponding effect at the rear end. This is because the occurrence of a reverse, stagnant, or forward flow within the channel is due to the interaction between the flow conditions at the front and rear ends. To see this interaction more clearly and to have a better understanding of the correspondence between the flow

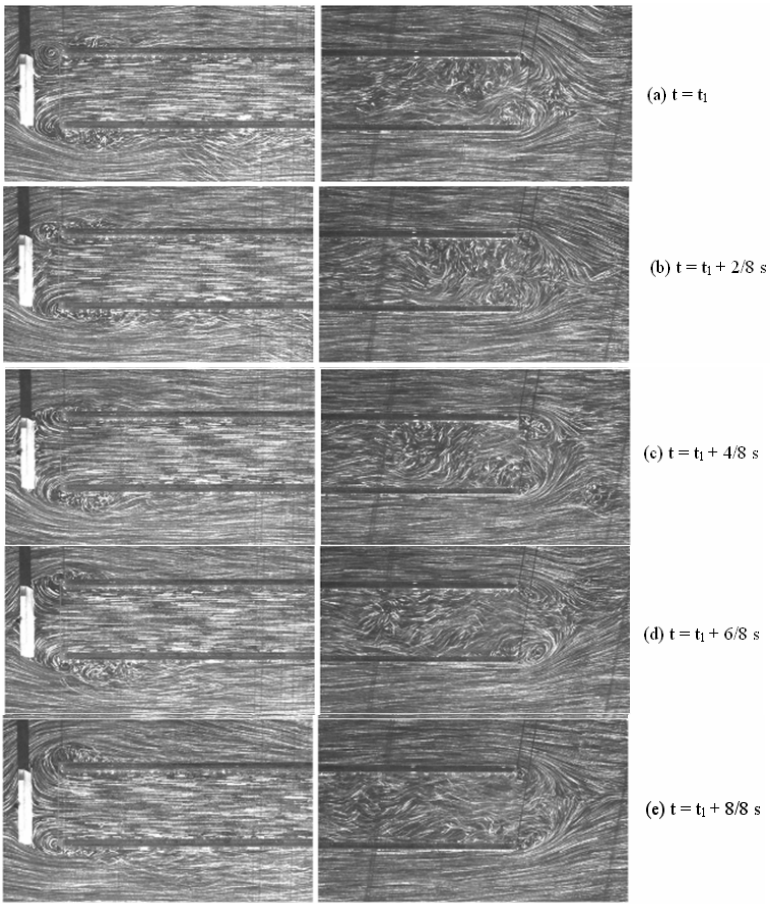

Fig. 8. Flow pattern at different instances (Re = 4,000, g/w = 0.5).

conditions at the front and rear ends as g/w is varied, the velocity profiles near the exit of the duct are examined. This is done for the region near the rear end where the shear layers curl up in response to the flow conditions at the front end. The profiles are shown for three typical values of g/w: (a) g/w = 1 (Fig. 10), when there is a strong reverse flow in the duct; (b) g/w = 1.75 (Fig. 11), when the flow is stagnant within the duct; and (c) g/w = 2 (Fig. 12) when forward flow occurs. In each of these figures, X is measured in the horizontal direction from the rear end of the duct and Y from the duct center, normal to X in the horizontal plane.

The velocity vectors at the rear end in Fig. 10(a) clearly show the strong curling of the flow into the duct, which results in the high magnitude of the reverse flow for this case (Fig. 7). The vector patterns on either side of the center are nearly symmetrical, which is also seen in the U-profiles shown in Fig. 10(b). A stagnation point occurs at a value of X/w between 0.577 and 0.769 as shown by the U-profiles. Beyond the stagnation point, the flow is in the forward direction and relaxes at what appears to be a rapid rate.

In Fig. 11(a), for g/w = 1.75, the flow pattern is different compared with that in Fig. 10(a). Here, it is seen that there are two recirculating regions that occur away from the duct exit, which appear to have a "sealing effect;" the vectors indicate very little flow into the duct. This and the vortical pattern at the front end (Fig. 6(e)) are the reasons for the stagnant conditions within the duct. The U-profiles shown in Fig. 11b reveal the low values of velocities; particularly for X/w = 0, the low values occur right across the cross section of the duct. The stagnation point (as revealed by the U-profiles) occurs around X/w = 1. The profiles beyond the stagnation point relax with increased distance from the exit of the duct. However,

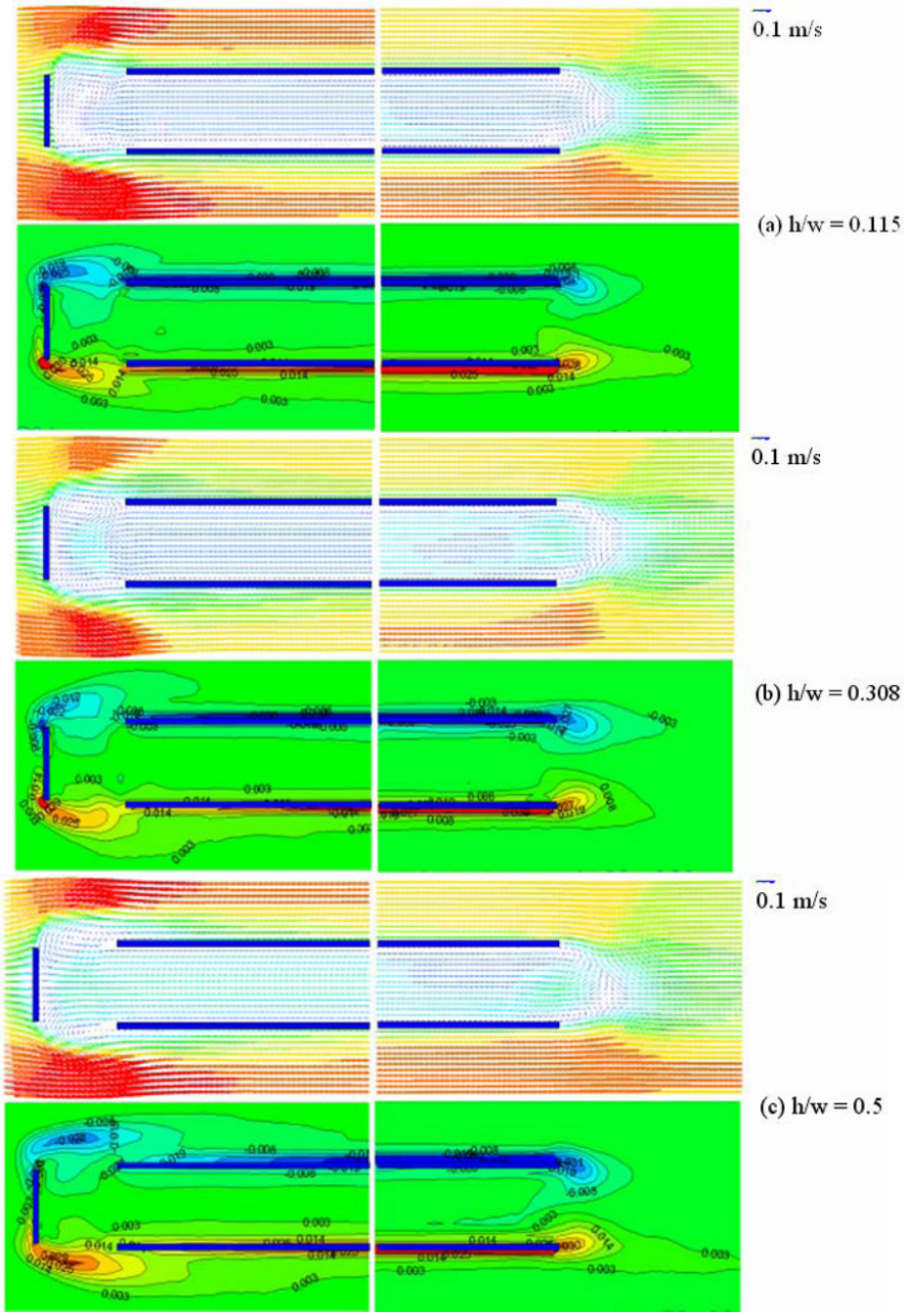

Fig. 9. Mean velocity vectors and vorticity contour at various heights (g/w = 1.0; Re = 4,000).

the relaxation appears to be slower compared with that seen for g/w = 1 (Fig. 10(b)). In addition, the symmetry of the profiles is weaker compared with the earlier case. The reason could be that, for this case, the flow is comparatively unsteady. As mentioned previously, for g/w = 1.75, the flow within the duct also showed some unsteadiness—sometimes slightly forward, sometimes slightly reverse, but overall stagnant.

The conditions shown in Fig. 12(a) for g/w = 2 re-

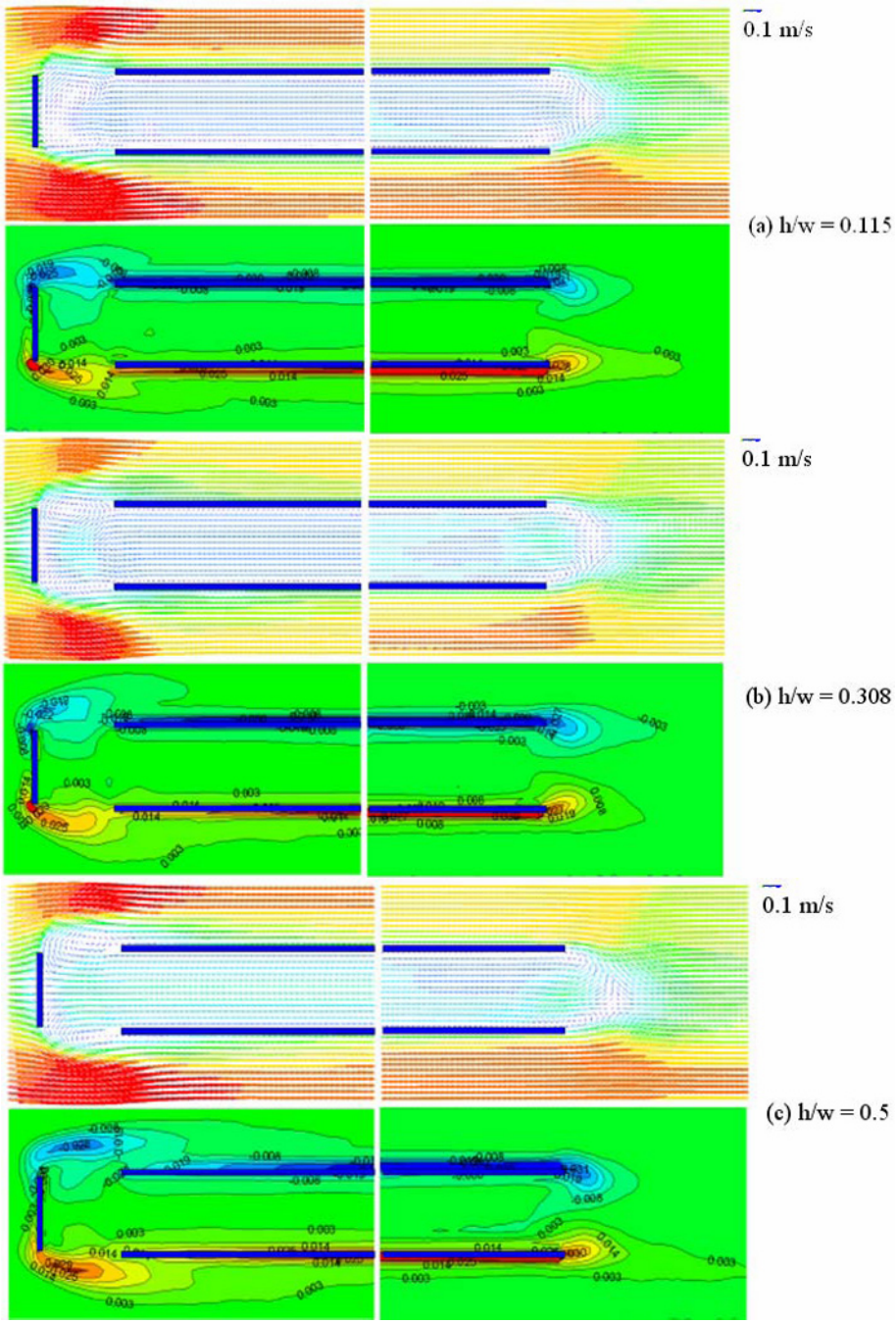

Fig. 9. Mean velocity vectors and vorticity contour at various heights (g/w = 1.0; Re = 4,000; continued).

veal that there is hardly any recirculation region at the rear end, though the velocity vectors indicate that the magnitudes change along the X direction. There is no stagnation point. The U-profiles in Fig. 12(b) show that the profiles up to X/w = 0.577 have a "top hat" shape with high velocity in the central region. For higher values of X/w, the shape changes considerably, becoming almost flatter and then relaxing like wake profiles. However, in this case, the relaxation is very slow compared with the profiles in Fig. 10(a) and Fig.

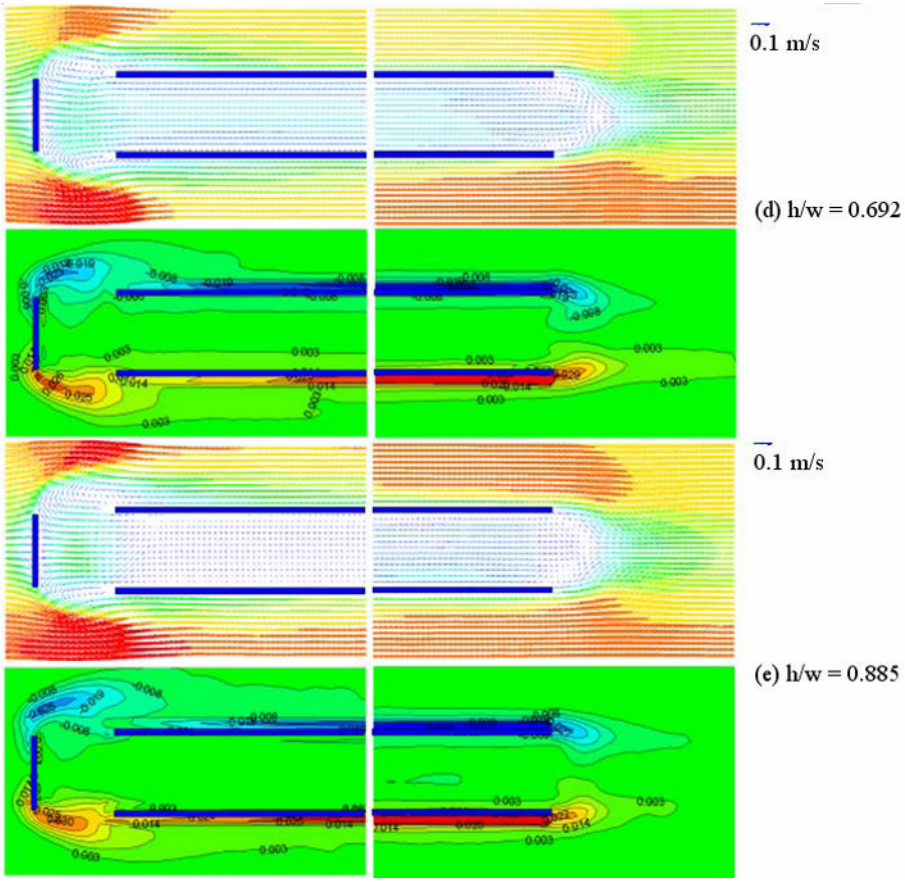

Fig. 9. Mean velocity vectors and vorticity contour at various heights (g/w = 1.0; Re = 4,000; continued).

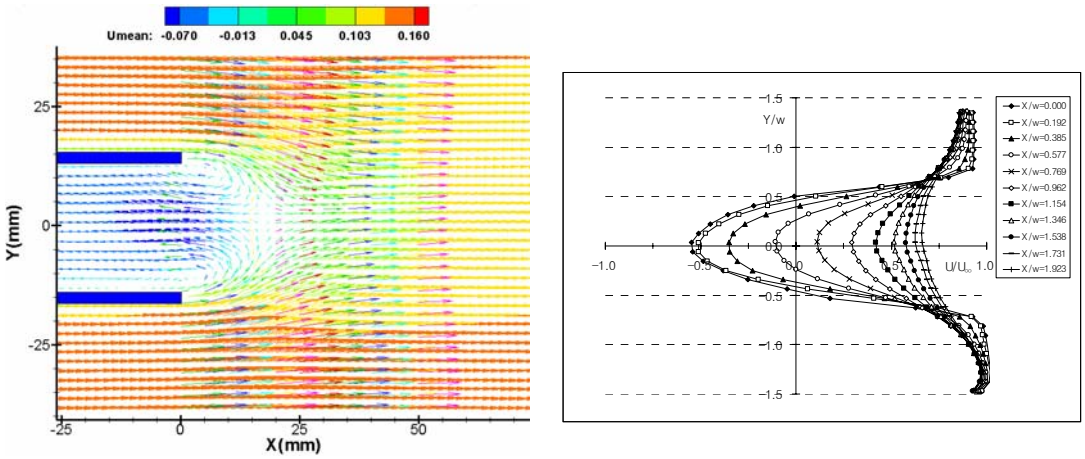

(a) Velocity vectors (b) U - profiles

Fig. 10. Velocity profiles at different distances from the end of the test duct (Re = 4,000, g/w = 1.0).

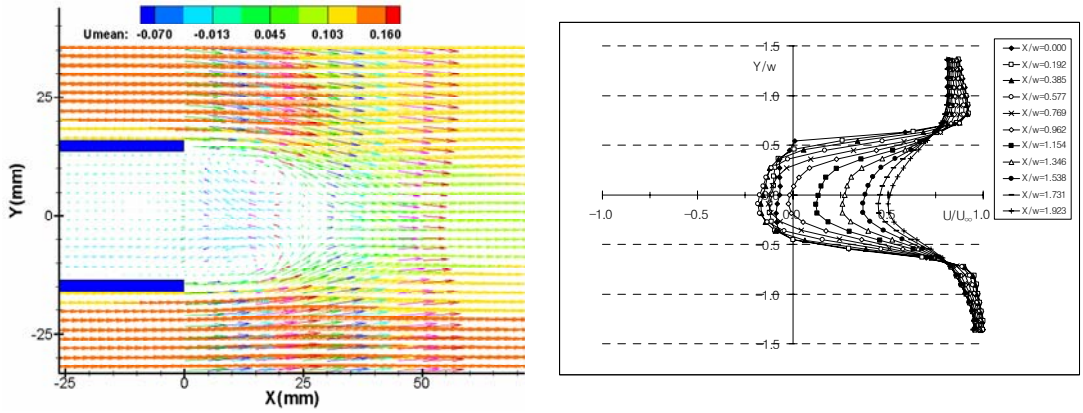

(a) Velocity vectors (b) U-profiles

Fig. 11. Velocity profiles at different distances from the end of the test duct (Re = 4,000, g/w = 1.75).

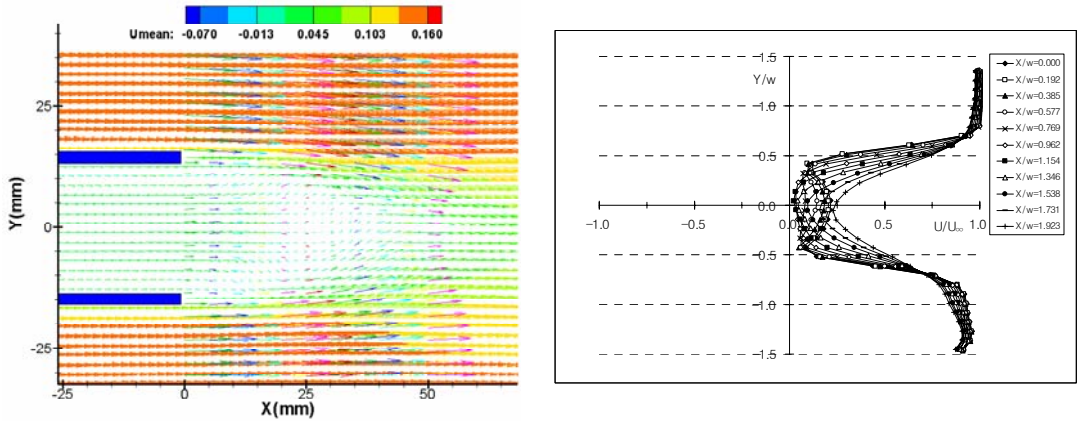

(a) Velocity vectors (b) U-profiles

Fig. 12. Velocity profiles at different distances from the end of the test duct (Re = 4,000, g/w = 2.0).

11(a). Even at X/w = 1.923, the velocity defect at the center (Y = 0) is considerably larger compared with the other two cases. It appears that for slow forward flow, the shear layers from the sides of the duct interact very slowly, and it would take a considerable distance downstream for this interaction to be completed.

The occurrence or non-occurrence of the stagnation point and its location seem to have a considerable influence on the structure of the flow at the rear end. To examine this, the location of the stagnation point for some typical values of g/w was determined by plotting the U values along X, at Y = 0, that is, along the center line from the rear end. Fig. 13 shows where the points of intersection of the curves with the horizontal axis for each value of g/w occurs which indicate the location of the stagnation point to a rea-

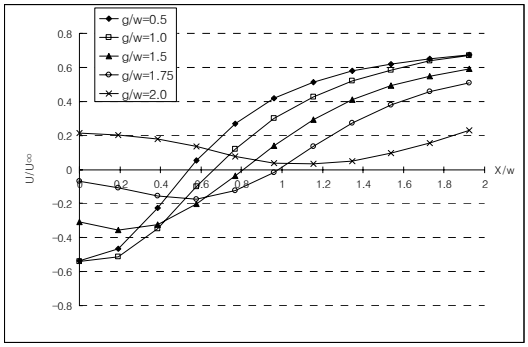

Fig. 13. Velocity at exit along Y/w = 0.0 for different g/w ratio (Re = 4,000).

sonable degree of accuracy. It can be seen that the location varies with g/w. For stagnant conditions (g/w = 1.75), it is located about one width away from the duct exit. At g/w = 2, the stagnation point is absent and no reverse flow occurs.

In light of the features discussed, the following can be stated: As the shear layers behind the obstruction at the front end roll up and adjust themselves depending on the gap between the obstruction and the duct entry, the flow at the rear end appears to respond by curling into the duct. Vortical patterns are thus formed and a stagnation point occurs at some distance away from the rear end. The position of the stagnation point seems to play an important role in deciding the magnitude of the reverse flow within the duct—low, high, or stagnant conditions. When forward flow occurs, the stagnation point disappears. Thus, it is very interesting to see the mutual response (communication) between the flow at the front and rear ends of the duct as g/w is varied.

Most of the results presented and discussed are restricted to a plane passing through the middle of the duct (except those in Fig. 9 where the results at cross sections are at various heights across the duct), though the flow configuration considered is three-dimensional. In spite of this limitation and in light of the features observed in Fig. 9, the results presented give a very reasonable picture of the three-dimensional flow considered.

5. Concluding remarks

Reverse flow occurs in a square duct when an obstruction is placed in front of the duct. The magnitude of the reverse flow is nearly twice that observed for the channel case. The PIV studies conducted have brought out the flow features responsible for these differences. Primarily, the interaction of the shear layers at the rear is quite different for the square duct; there is no alternate pumping of fluid (unlike for a channel) but a continuous flow into the duct in the reverse direction. A vortex ring-like structure can be expected at the rear end. The maximum reverse flow is nearly twice that for the channel case and occurs at a g/w value of 0.75. The increase in the magnitude of the reverse flow compared with the channel case appears to be mainly due to the geometry of the duct. However, the values of g/w at which maximum reverse flow occurs, stagnant conditions prevail, and forward flow begins seem to be decided by the geometry of the obstruction.

Acknowledgement

This work was supported by the Grant of the Korean Ministry of Education, Science and Technology (The Regional Core Research Program).

Nomenclature

B : Side width of the square plate obstruction
G : Gap between the obstruction and the duct entry
H : Distance from one end of the duct indicating the height of the cross section
L : Length of the duct
U : Mean velocity in the X direction
U_i : Mean velocity within the duct
U_∞ : Free stream velocity
X : Distance along the horizontal direction measured from the rear end of the duct
Y : Distance measured from the center of the duct normal to the X direction in the horizontal plane
w : Side width of the square duct

References

[1] M. A. Bhuiyan, M. M. A. Khan and M. A. Kabir, Reverse flow of a non-Newtonian fluid in a channel, *Proc. Rheology* Congress, Cambridge, UK, 3 (2000) 417-418.
[2] B. H. L. Gowda and E. G. Tulapurkara, Reverse flow in a channel with an obstruction at the entry, *Journal of Fluid Mechanics* 204 (1989) 229-244.
[3] B. H. L. Gowda, E. G. Tulapurkara and S. K. Swain, Reverse flow in a channel-influence of obstruction geometry, *Experiments in Fluids* 16 (1993) 137-145.
[4] E. G. Tulapurkara, B. H. L. Gowda and S. K. Swain, Reverse flow in a channel-effect of front and rear obstructions, *Physics of Fluids* 6 (1994) 3847-3853.
[5] B. H. L. Gowda, E. G. Tulapurkara and S. K. Swain, Influence of splitter plate on the reverse flow in a channel, *Fluid Dynamics Research* 21 (1997) 319-330.
[6] B. H. L. Gowda, E. G. Tulapurkara and S. K. Swain, On the mechanism of reverse flow in a channel with an obstruction at the entry, *Fluid Dynamics Research* 23 (1998) 177-187.
[7] M. A. Kabir, M.M.A. Khan and M. A. Bhuiyan, A study of the flow phenomenon in water in a channel with flat plate obstruction geometry at the entry,

KSME Int. Journal 17 (2003) 879-887.

[8] M. A, Kabir, M. M. A. Khan and M. A. Bhuiyan, Flow phenomenon in a channel with differently shaped obstructions at the entrance, *Fluid Dynamics Research* 35 (2004) 395-408.

[9] C. H. Sohn, Y. Z. Zhang and B. H. L. Gowda, Reverse flow in a circular duct with an obstruction at the entry, *Flow Measurement and Instrumentation* 18 (2007) 230-234.

Chang Hyun Sohn received M.Sc. (Eng) and Ph.D. from KAIST. He worked in ADD for 3 years. He studied in Cambridge University as a visiting assistant professor from 1996 to 1997. He is a full professor to the school of mechanical engineering, Kyungpook National University. His research interests are CFD, PIV, Flow Induced Vibration and Thermal-hydraulics in Mechanical Engineering Field.

B. H. Lakshmana Gowda: He received his M.E. (Eng) in 1965 from Indian Institute of Science, Bangalore. He also received his Ph.D. in 1974 from Indian Institute of Technology, Madras. He worked in Indian Institute of Technology, Madras as a professor since 1967. He worked in Kyungpook National University as a visiting professor from 2004. He works in Mechanical Engineering, BTL Institute of Tecnology, Bommasandra, Bangalore since 2008. His research interests are Turbulent Shear Flows, Flow Induced Vibration and Flow Around Three-Dimensional Bluff Bodies.

Myoung Gun Ju: He received his M. Sc. (Eng) in Mechanical Engineering in 2009 from Kyoungpook National University.